nature immunology

MicroRNA miR-326 regulates T_H-17 differentiation and is associated with the pathogenesis of multiple sclerosis

Changsheng Du[1,5], Chang Liu[1,5], Jiuhong Kang[1,2], Guixian Zhao[3], Zhiqiang Ye[4], Shichao Huang[1], Zhenxin Li[3], Zhiying Wu[3] & Gang Pei[1,2]

Interleukin 17 (IL-17)-producing T helper cells (T_H-17 cells) are increasingly recognized as key participants in various autoimmune diseases, including multiple sclerosis. Although sets of transcription factors and cytokines are known to regulate T_H-17 differentiation, the role of noncoding RNA is poorly understood. Here we identify a T_H-17 cell–associated microRNA, miR-326, whose expression was highly correlated with disease severity in patients with multiple sclerosis and mice with experimental autoimmune encephalomyelitis (EAE). *In vivo* silencing of miR-326 resulted in fewer T_H-17 cells and mild EAE, and its overexpression led to more T_H-17 cells and severe EAE. We also found that miR-326 promoted T_H-17 differentiation by targeting Ets-1, a negative regulator of T_H-17 differentiation. Our data show a critical role for microRNA in T_H-17 differentiation and the pathogenesis of multiple sclerosis.

After antigen stimulation, naive $CD4^+$ helper T cells differentiate into effector T cells to participate in the adaptive immune response. Interleukin 17 (IL-17)-producing T helper cells (T_H-17 cells) have been identified as a distinct subset of effector helper T cells that are essential in clearing foreign pathogens and inducing tissue inflammation during autoimmune disease[1,2]. T_H-17 differentiation is directed by lineage-specific transcription factors, including RORγt and RORα[3], and is controlled by the coordinated activity of a series of positive and negative regulators[4–7]. Although the list of molecular regulators of T_H-17 differentiation is ever growing, possible factors that link the generation of T_H-17 cells to pathological conditions, such as autoimmunity, are largely unknown and need to be clarified.

As a prototype of organ-specific autoimmune disease, multiple sclerosis is manifested by chronic inflammatory demyelination of the central nervous system (CNS) and is one of the foremost causes of nontraumatic neurological disability in young adults[8,9]. The disease is clinically heterogeneous, with about 80% of patients developing the relapsing-remitting multiple sclerosis (RRMS) subtype[10]. Because of limited understanding of the pathogenesis of multiple sclerosis and a lack of sensitive biomarkers, according to the present criteria[11], the diagnosis of multiple sclerosis still depends on repeated occurrence of the disease. In addition, the signs and symptoms of multiple sclerosis usually share considerable similarity with those of other CNS inflammatory diseases, such as neuromyelitis optica (NMO); this leads to considerable therapeutic and diagnostic difficulties. $CD4^+$ T cell–mediated autoimmunity has long been accepted as one of the most important aspects of multiple sclerosis pathogenesis, especially for the early initiation of disease[12,13]. T helper type 1 (T_H1) cells, characterized by the production of interferon-γ (IFN-γ), have been considered the type of effector helper T cells that mediate the pathogenesis of multiple sclerosis; subsequent studies have indicated that T_H-17 cells are involved and are at least as critical as T_H1 cells in this pathogenesis. Mice with fewer T_H-17 cells are less susceptible to experimental autoimmune encephalomyelitis (EAE)[14,15], and IL-17-expressing T cells have been found in lesions of brain tissues from patients with multiple sclerosis[16]. Despite the lines of evidence described above, the underlying mechanisms of T_H-17 differentiation, as well as potential clinical applications, including the identification of T_H-17-related diagnosis markers or the development of T_H-17-targeting therapeutic approaches for multiple sclerosis, have not been established.

MicroRNAs represent a large family of endogenous noncoding RNAs that comprise a fundamental layer of post-transcriptional regulation of gene expression[17]. When poorly regulated, microRNAs are critically involved in a range of human diseases[18,19] and potentially serve as good diagnostic markers[20], prognostic markers[21] or therapeutic targets[19]. MicroRNAs also participate in the regulation of autoimmunity: deficiency in Dicer or Drosha leads to autoimmune signs in mice[22,23]. However, which microRNAs are involved in the regulation and control of autoimmune disease is unclear.

[1]Laboratory of Molecular Cell Biology, Institute of Biochemistry and Cell Biology, Shanghai Institutes for Biological Sciences, Graduate School of the Chinese Academy of Sciences, Chinese Academy of Sciences, Shanghai, China. [2]School of Life Science and Technology, Tongji University, Shanghai, China. [3]Department of Neurology and Institute of Neurology, Huashan Hospital, Shanghai Medical College, Shanghai, China. [4]Key Laboratory of Systems Biology, Shanghai Institutes for Biological Sciences, Chinese Academy of Sciences, Shanghai, China. [5]These authors contributed equally to this work. Correspondence should be addressed to G.P. (gpei@sibs.ac.cn).

Received 8 May; accepted 2 September; published online 18 October 2009; doi:10.1038/ni.1798

Table 1 Characteristics of patients and controls

	Control	RRMS	NMO
Sample size	42	43	11
Age	44 ± 12.0	39.6 ± 12.7	42.1 ± 13.4
Sex			
Female	20 (47.6%)	21 (48.8%)	7 (63.6%)
Male	22 (52.4%)	22 (51.2%)	4 (36.4%)
Clinical stage			
Relapsing	–	25	5
Remitting	–	18	6
Drug treatment	–	–	–

Relevant information about human subjects recruited for this study. Sample size is total number of subjects; age is presented in years ± s.e.m.; sex is total number (with percent of group in parentheses); '–' indicates 'not applicable'.

Here we report that the microRNA miR-326 is critical in regulating T_H-17 differentiation and hence contributes to the pathogenesis of multiple sclerosis. We found that miR-326 mediated T_H-17 differentiation through translational inhibition of Ets-1 (A000889), a negative regulator of T_H-17 differentiation. Knockdown or overexpression of miR-326 alleviated or aggravated EAE, respectively. In human patients with multiple sclerosis, miR-326 expression was upregulated, and this correlated with disease severity and IL-17 production. Collectively our results suggest that miR-326 is a T_H-17 cell–associated microRNA that functions in the pathogenesis of multiple sclerosis.

RESULTS

Upregulation of miR-326 in patients with multiple sclerosis

By using clinical samples (**Table 1**), we found that miR-326 expression was significantly higher in peripheral blood leukocytes (PBLs) of patients with RRMS (**Fig. 1a**) than in those of age-matched controls or patients with NMO, an inflammatory demyelinating CNS disease with symptoms that considerably overlap those of multiple sclerosis but an etiology distinct from that of multiple sclerosis[24]. Detailed analysis showed that PBLs from patients with relapsing multiple sclerosis had significantly higher miR-326 expression but those from patients with remitting multiple sclerosis did not (**Fig. 1b**). In contrast, the expression of seven known immunologically relevant microRNAs showed no substantial changes (**Supplementary Fig. 1**), which suggested a specific association of miR-326 expression with relapsing multiple sclerosis. More notably, there was even more prominently enhanced miR-326 expression in the $CD4^+$ T cell population but not in the $CD8^+$ T cell or non–T cell populations of patients with multiple sclerosis (**Fig. 1c**).

$CD4^+$ T cells that participate in multiple sclerosis pathogenesis take on the phenotype of T_H1 cells, T_H2 cells, T_H-17 cells or regulatory

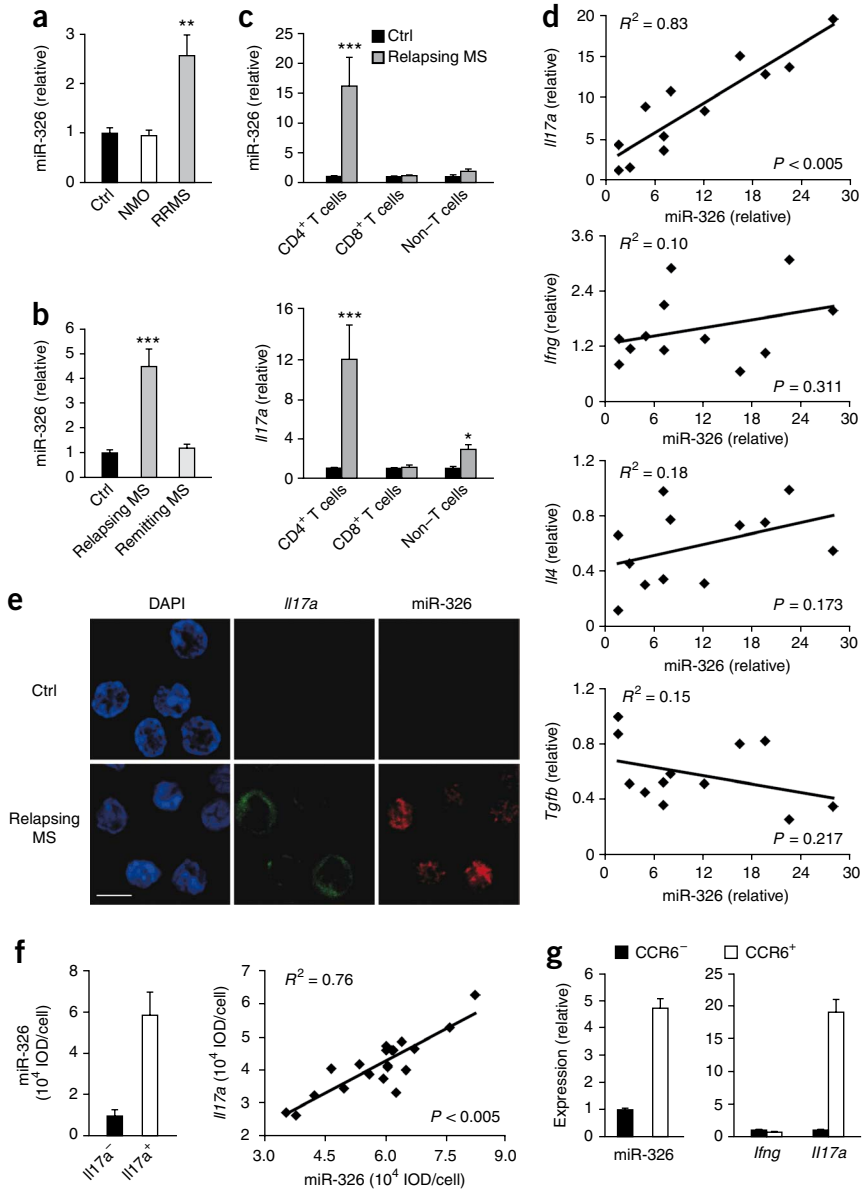

Figure 1 Upregulation of miR-326 in patients with multiple sclerosis. (**a**,**b**) Quantitative PCR analysis of miR-326 expression in PBLs from normal controls (Ctrl; $n = 42$) and patients with NMO ($n = 11$) or RRMS ($n = 43$; **a**) and PBLs from patients with relapsing multiple sclerosis ($n = 25$) or remitting multiple sclerosis ($n = 18$; **b**). MS, multiple sclerosis. (**c**) Expression of miR-326 and *Il17a* in $CD4^+$ T cells, $CD8^+$ T cells and the non–T cell fraction of PBLs from patients with relapsing multiple sclerosis and controls ($n = 7$ per group). (**d**) Linear correlation between transcripts of miR-326 and various cytokines in $CD4^+$ T cells from patients with RRMS ($n = 12$). (**e**) FISH analysis of transcripts of miR-326 and *Il17a* in $CD4^+$ T cells from patients with relapsing multiple sclerosis and normal controls. DAPI, DNA-intercalating dye (4,6-diamidino-2-phenylindole). Scale bar, 3 μm. (**f**) Quantification of the miR-326 and *Il17a* signals in **e**. IOD, integrated optical density. (**g**) Expression of miR-326, *Ifng* and *Il17a* in $CCR6^+$ and $CCR6^-$ populations sorted from multiple sclerosis $CD4^+$ T cells ($n = 3$). Results in **a**–**d**,**g** are normalized to those of controls and are presented relative to expression of the small nuclear RNA RNU6B (for miR-326) or the 'housekeeping' gene *Rpl13a* (for cytokines; encodes the ribosomal protein L13A). $^*P < 0.05$, $^{**}P < 0.01$ and $^{***}P < 0.005$, versus control (Student's *t*-test). Data are representative of two independent experiments (mean and s.e.m. in **a**–**d**,**g**).

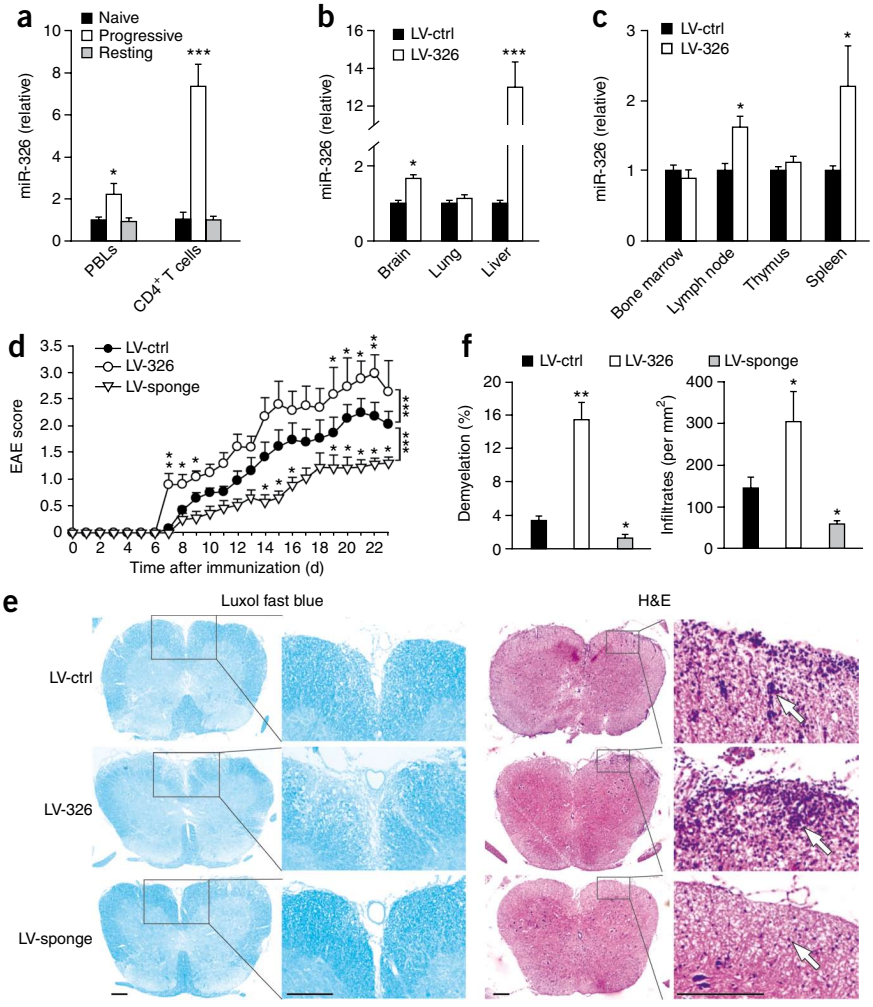

Figure 2 Regulation of EAE development by miR-326. (**a**–**c**) Quantitative PCR analysis of miR-326 expression in PBLs and $CD4^+$ T cells during EAE development ($n = 6$ mice per group; **a**) or from the brain, lung and liver (**b**) or bone marrow, peripheral lymph nodes, thymus and spleen (**c**) of mice infected with LV-326 or LV-ctrl (day 7 after lentivirus administration; $n = 3$ mice per group). Results are normalized to those from naive mice (**a**) or LV-ctrl mice (**b**,**c**) and are presented relative to RNU6B results. (**d**) Clinical scores for EAE in mice infected with lentivirus ($n = 9$–10 mice per group). (**e**) Histology of paraffin sections of spinal cords isolated from lentivirus-infected mice ($n = 3$ mice per group) on day 21 after immunization. Arrows indicate inflammatory infiltrations; boxed areas in left columns are presented enlarged at right. H&E, hematoxylin and eosin. Scale bars, 70 μm. (**f**) Quantification of demyelination and spinal cord infiltrates in the sections in **f**, presented as demyelination area relative to total analyzed area (left) and infiltrates per mm^2 (right). $^*P < 0.05$, $^{**}P < 0.01$ and $^{***}P < 0.005$, versus control (Student's *t*-test (**a**–**c**,**e**) or two-way analysis of variance followed by Bonferroni's post-hoc test (parametric data) or Mann–Whitney test (nonparametric data; **d**)). Data are from two (**a**–**c**,**e**,**f**) or four (**d**) independent experiments (mean and s.e.m., **a**–**d**,**f**).

T cells (T_{reg} cells), which are specialized in the production of IFN-γ, IL-4, IL-17 or transforming growth factor-β (TGF-β), respectively. We investigated which helper T cell subset was associated with miR-326 upregulation in patients with multiple sclerosis. Expression of *Il17a*, but not of *Ifng*, *Il4* or *Tgfb*, increased with miR-326 expression (**Fig. 1c** and **Supplementary Fig. 2**). We further confirmed the upregulation of *Il17a* in patients with relapsing multiple sclerosis at the protein level by intracellular cytokine staining of $CD4^+$ T cells (**Supplementary Fig. 3**). Linear correlation analysis of transcripts of miR-326 and those cytokines in $CD4^+$ T cells for patients with RRMS further demonstrated that only *Il17a* expression correlated well with that of miR-326 (**Fig. 1d**). Consistent with that, by fluorescence *in situ* hybridization (FISH), we found coexpression of miR-326 and *Il17a* in $CD4^+$ T cells of patients with relapsing multiple sclerosis (**Fig. 1e**,**f**), which showed that miR-326 was expressed in the T_H-17 cell population. This was further confirmed by the high expression of miR-326 in $CCR6^+CD4^+$ PBLs of patients with relapsing multiple sclerosis (**Fig. 1g**), a population that identifies most human T_H-17 cells[25]. These results demonstrate that T_H-17 cells have high expression of miR-326 and that miR-326 expression significantly correlates with multiple sclerosis severity.

Regulation of EAE development by miR-326

Expression of miR-326 was also higher in $CD4^+$ T cells from mice with EAE during the acute phase but decreased to normal expression when disease remitted (**Fig. 2a**), similar to what occurs in patients with RRMS. To investigate whether manipulation of miR-326 can influence the development of EAE, we constructed lentiviral vectors for *in vivo* miR-326 manipulation. We designed vectors encoding pre-miR-326 (LV-326), a mutant miR-326 control (LV-ctrl) or its specific inhibitor (LV-sponge) and confirmed overexpression or active inhibition of miR-326, respectively (**Supplementary Fig. 4** and **Supplementary Methods**). The term 'sponge' refers to a miR-326-specific decoy target known to suppress endogenous miR-326 activity without affecting its transcript amounts[26]. We delivered approximately 2×10^7 transforming units of recombinant lentivirus to mice by injection through the tail vein and assessed the *in vivo* efficacy of lentivirus infection 7 d later by quantitative PCR analysis of miR-326 expression in various organs (including those of the immune system) of LV-326-infected mice and LV-ctrl-infected mice. Consistent with published reports[27], systemic administration of lentivirus led to differences in expression of the transgene among various organs, with the liver being most susceptible and the brain or lungs being least accessible to the virus (**Fig. 2b**). In organs related to the immune system, infection with LV-326 led to two-fold greater expression of mature miR-326 in spleen and 1.6-fold greater expression in the peripheral lymph nodes (subiliac, proper axillary and accessory axillary), but we detected little miR-326 overexpression in bone marrow or thymus (**Fig. 2c**). Notably, the peripheral T lymphocyte and B lymphocyte population and $CD4^+$ T cell/$CD8^+$ T cell ratio in the resting state showed no difference among mice infected with those lentiviruses (**Supplementary Fig. 5**), nor did we find substantial differences between naive ($CD62L^+CD44^{lo}CD4^+$) T cells and antigen-experienced ($CD62L^-CD44^{hi}CD4^+$) T cells (data not shown), which indicates that miR-326 might not affect

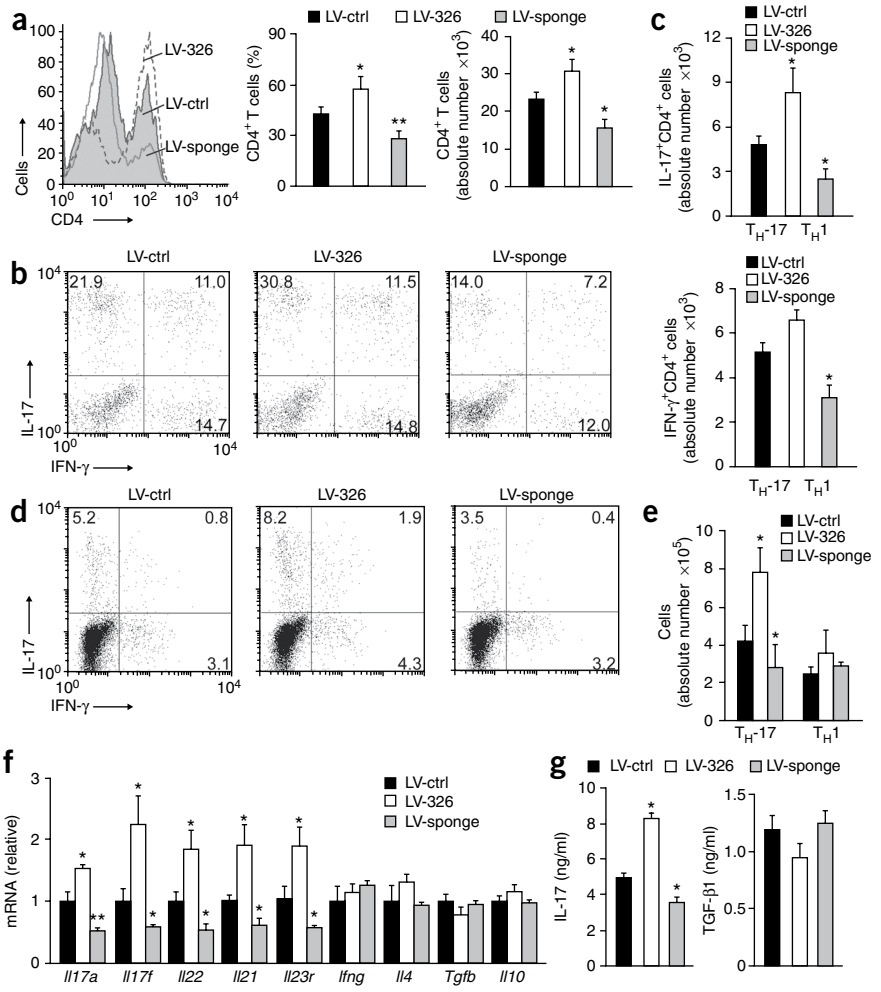

Figure 3 *In vivo* generation of T_H-17 cells in EAE mice is enhanced by miR-326. (**a**) Quantification of CD4+ T cells in mononuclear cell infiltrates isolated from brains and spinal cords of lentivirus-infected mice on day 21 after immunization. (**b**) Intracellular staining of IL-17 and IFN-γ in the cells in **a**. Numbers in quadrants indicate percent cells in the CD4+ gate. (**c**) Absolute number of CD4+IL-17+ (T_H-17) cells and CD4+IFN-γ+ (T_H1) cells analyzed in **b**. (**d**) Intracellular staining of IL-17 and IFN-γ in DLN cells isolated from lentivirus-infected mice on day 14 after immunization. Numbers in quadrants indicated percent CD4+ cells. (**e**) Absolute number of T_H-17 and T_H1 cells in **d**. (**f**) Quantitative PCR analysis of gene expression in the DLN cells in **d**, presented relative to *Rpl13a* expression. (**g**) IL-17 and TGF-β1 in supernatants of DLN cells restimulated *in vitro* with MOG (35–55; 20 μg/ml) and assessed at 48 h of culture. $^*P < 0.05$ and $^{**}P < 0.01$, versus control (Student's *t*-test). Data are from three independent experiments (mean and s.e.m. in **a**,**c**,**e**,**f**).

the homeostasis of the T lymphocyte and B lymphocyte repertoire in naive mice.

After immunization of lentivirus-infected mice with an encephalitogenic peptide of myelin oligodendrocyte glycoprotein consisting of amino acids 35–55 (MOG(35–55)) on day 7 after virus injection, LV-326-infected mice developed severe EAE, whereas LV-sponge-infected mice had somewhat mild EAE, both relative to that of LV-ctrl-infected mice (**Fig. 2d** and **Table 2**). Histological analysis of spinal cord sections also showed that LV-326-infected mice developed prominent inflammatory infiltration and demyelination, whereas LV-sponge-infected mice showed mild CNS pathology (**Fig. 2e**,**f**). To conclusively demonstrate that miR-326 is critical in EAE development, we first sought to further verify the expression and distribution of the lentiviral transgene in the EAE mice. Because of the low multiplicity of infection (<1) limited to systemic lentiviral administration and the resultant very weak fluorescence of green fluorescent protein (GFP) for measurement, we did sensitive FISH analysis of GFP transcripts (**Supplementary Methods**). We found that the proportion of virus-infected cells in total cell populations of PBLs, spleens, draining lymph nodes (DLNs; pooled peripheral lymph nodes from subiliac, proper axillary and accessory axillary lymph nodes) and CNS infiltrates from virus-infected mice with EAE was 45%, 39%, 33% and 51% respectively (**Supplementary Fig. 6a–e**). Notably, the highest transduction efficiency was in the CNS infiltrates of mice with EAE, which supports the idea that lentivirus-mediated manipulation of miR-326 contributes to altered EAE pathology.

Table 2 EAE in lentivirus-infected mice

Group	Incidence	Time of onset	Maximum score	Score > 3
LV-ctrl	10 of 10	6.9 (± 0.2)	2.2 (± 0.3)	4 of 10
LV-326	9 of 9	6.3 (± 0.2)	3.6 (± 0.3)*	7 of 9
LV-sponge	10 of 10	7.7 (± 1.2)	1.4 (± 0.2)*	1 of 10

Development of EAE in lentivirus-infected mice immunized with MOG (35–55) emulsified in complete Freund's adjuvant. Incidence indicates number of mice that developed EAE relative to total mice in group; time of onset is presented in days (mean ± s.e.m.); maximum EAE score is presented as mean (± s.e.m.); far right column is the number of mice achieving an EAE score of greater than 3 relative total mice in group. $^*P < 0.05$, versus control (Student's *t*-test). Data are cumulative results from four different experiments.

Further analysis showed that the specific transduction efficiency in CD4+ T cells, CD8+ T cells and B cells, quantified by the percentage of positive infection in each cell subset, was around 50%, 33% and 28% respectively (as averaged for PBLs, spleen, DLNs and CNS infiltrates; **Supplementary Fig. 6a–d**,**f**), which showed the relative selectivity of lentivirus infection for CD4+ T cells. There was no obvious difference in the transduction efficiency of naive and effector CD4+ T cells (**Supplementary Fig. 7a**,**c**). Moreover, we also confirmed these data by flow cytometry (**Supplementary Figs. 7b**,**c** and **8**). The data presented above collectively showed that EAE pathology differed greatly in mice efficiently infected by miR-326 or lentivirus encoding its inhibitor, which demonstrated that miR-326 expression and function correlated with the development of EAE.

Promotion of T_H-17 differentiation by miR-326

We then sought to determine whether the difference in EAE pathology in the three groups of lentivirus-infected mice was associated with altered infiltration of the CNS with effector helper T cells (mainly T_H-17 and T_H1 cells), a hallmark of CNS inflammation in EAE. More CD4+ T cells accumulated in the CNS of LV-326-infected mice, whereas fewer CD4+ T cells were present in mice infected with LV-sponge, as measured by CD4 surface staining of

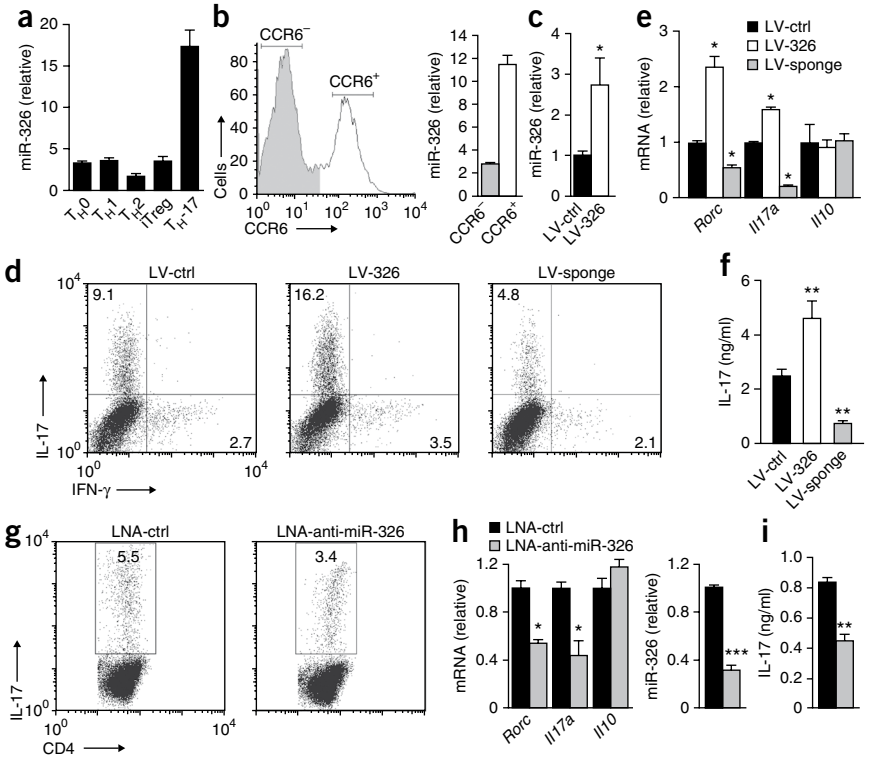

Figure 4 Promotion of *in vitro* T_H-17 differentiation by miR-326. (**a**–**c**) Quantitative PCR analysis of miR-326 expression in T_H0, T_H1, T_H2, T_H-17 and inducible T_{reg} cells differentiated *in vitro* (**a**), flow cytometry–sorted (left) CCR6$^+$CD4$^+$ and CCR6$^-$CD4$^+$ T cells from *in vitro* T_H-17 cultures (**b**), and purified naive CD4$^+$CD62L$^+$ T cells of lentivirus-infected mice (**c**; $n = 2$ mice per group); results are presented relative to RNU6B expression. (**d**–**f**) Intracellular staining of IL-17 (**d**), quantitative PCR analysis of the expression of *Rorc*, *Il17a* and *Il10* (**e**) and enzyme-linked immunosorbent assay (ELISA) of IL-17 in culture supernatants (**f**) of naive CD4$^+$CD62L$^+$ T cells obtained from lentivirus-infected mice and cultured for 4 d in T_H-17-polarizing conditions. Numbers in quadrants (**d**) indicate percent IL-17$^+$IFN-γ$^-$ cells (top left) or IL-17$^-$IFN-γ$^+$ cells (bottom right). (**g**–**i**) Intracellular staining of IL-17 (**g**), quantitative PCR analysis of the expression of *Rorc*, *Il17a*, *Il10* and miR-326 (**h**) and ELISA of IL-17 in culture supernatants (**i**) of naive C57BL/6 CD4$^+$CD62L$^+$ T cells cultured for 20 h in 'T_H0' conditions (antibody to IL-4 (anti-IL-4) plus anti-IFN-γ but no additional cytokines) and transfected by nucleofection with the microRNA inhibitor LNA-anti-miR-326 or 'scrambled' control antisense oligonucleotide (LNA-ctrl), followed by T_H-17 polarization for another 4 d. Numbers in outlined areas (**g**) indicate percent IL-17$^+$ cells in the CD4$^+$ gate. $^*P < 0.05$, $^{**}P < 0.01$ and $^{***}P < 0.005$, versus control (Student's *t*-test). Data are from three (**a**,**b**,**g**–**i**) or two (**c**–**f**) experiments (mean and s.e.m., **a**–**c**,**e**,**f**,**h**,**i**).

CNS leukocyte infiltrates (**Fig. 3a**). Intracellular cytokine staining showed that both the frequency and absolute number of T_H-17 cells, but not of T_H1 cells, in the CD4$^+$ population were higher in LV-326-infected mice but lower in LV-sponge-infected mice (**Fig. 3b**,**c**). We also investigated the correlation between IL-17 production and virus infection in CNS by FISH analysis of *Il17a* and the sequence encoding GFP. This showed that the percentage of IL-17-producing cells in the GFP$^+$ population was higher in CNS infiltrates from LV-326-infected mice but lower in those from LV-sponge-infected mice. In contrast, the percentage of IL-17-producing cells was similar among GFP$^-$ cells in all samples examined (**Supplementary Fig. 9**). These data collectively indicate that miR-326 functions in EAE development largely by affecting the T_H-17 cell population.

Next we examined effector T cells primed in peripheral lymph nodes from EAE mice in which miR-326 expression had been manipulated. We found more T_H-17 cells in DLNs of LV-326-infected mice and fewer in those of LV-sponge-infected mice than in those of control mice. In contrast, T_H1 cell numbers were similar in the various groups of mice (**Fig. 3d**,**e**). Consistent with that, genes specific for the T_H-17 lineage, including *Il17a*, *Il17f*, *Il22*, *Il21* and *Il23r*, were significantly upregulated in LV-326-infected mice and downregulated in LV-sponge-infected mice, whereas genes related to other helper T cell subsets, such as *Ifng*, *Il4* and *Tgfb*, were unchanged in LV-326- and LV-sponge-infected mice relative to their expression in LV-ctrl-infected mice (**Fig. 3f**). Antigen-specific T_H-17 responses in DLN cells from LV-326- or LV-sponge-infected mice were higher and lower, respectively, as shown by measurement of IL-17 in culture supernatants of DLN cells after *in vitro* restimulation with MOG (35–55) (**Fig. 3g**). Production of the T_{reg} cell–related cytokine TGF-β was not obviously affected by miR-326 (**Fig. 3g**). In addition, IL-17 expression in CD8$^+$ T cells as well as in γδ T cells did not differ among mice infected with LV-ctrl, LV-326 or LV-sponge (**Supplementary Fig. 10**). Collectively these data suggest that miR-326 regulates the *in vivo* generation of T_H-17 cells during EAE.

To directly assess if miR-326 regulated the differentiation of T_H-17 cells, we did an *in vitro* T cell–differentiation assay. By comparing miR-326 expression in all subsets of helper T cells with that in naive CD4$^+$ T cells, we found large amounts of miR-326 (17.4-fold more than that in naive CD4$^+$ T cells) 'preferentially' in T_H-17 cells but relatively small and similar amounts in T_H1, T_H2 and inducible T_{reg} cells (about 1.6-fold to 3.3-fold more than that in naive CD4$^+$ T cells; **Fig. 4a**). As a control for *in vitro* differentiation, we measured lineage-specific transcription factors and cytokines (**Supplementary Fig. 11a**,**b**). CCR6$^+$ cells from *in vitro* T_H-17 cell cultures had approximately fivefold higher miR-326 expression than did their CCR6$^-$ counterparts (**Fig. 4b**), along with the enrichment of *Il17a* expression (**Supplementary Fig. 11c**). Again these data indicated that miR-326 expression is associated with mouse T_H-17 cells as with human T_H-17 cells. We then purified naive CD4$^+$CD62L$^+$ helper T cells from spleens of mice infected with LV-ctrl, LV-326 or LV-sponge and primed the cells for T_H-17 differentiation *in vitro*. We found 2.5-fold more miR-326 expression in T cells from LV-326-infected mice (**Fig. 4c**). More T_H-17 cells were produced by naive CD4$^+$ T cells from LV-326-infected mice and fewer were produced by those from LV-sponge-infected mice (**Fig. 4d**). The expression of T_H-17-lineage marker genes (*Rorc* and *Il17a*) and IL-17 in culture supernatants were also greater with miR-326 overexpression. In contrast, these T_H-17 lineage markers were downregulated in T cells from LV-sponge-treated mice after culture in the same conditions (**Fig. 4e**,**f**). Expression of IL-10, an anti-inflammatory cytokine also induced by T_H-17 cells, however, was not affected by miR-326 expression (**Fig. 4e**). The broadly

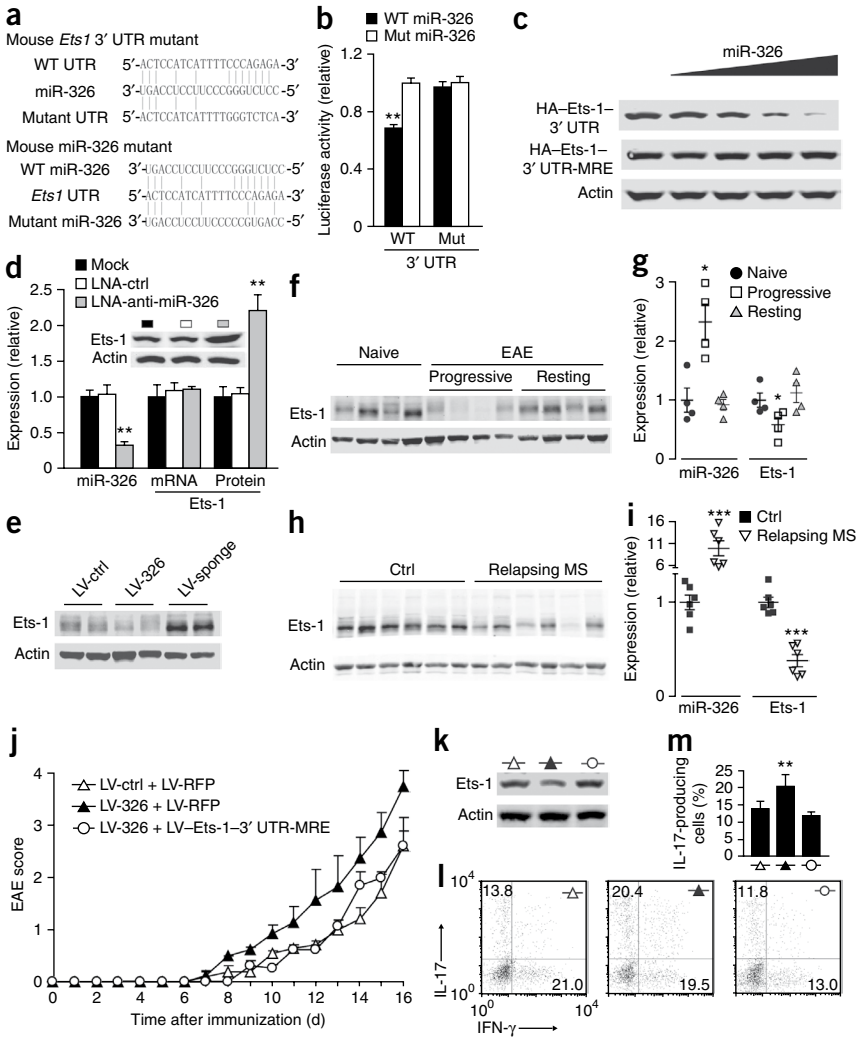

Figure 5 Ets-1 is a functional target of miR-326. (**a**) Mutations in the *Ets1* 3′ UTR (top) and miR-326 (bottom). (**b**) Luciferase activity of reporter carrying the mutated (Mut) or wild-type (WT) *Ets1* 3′ UTR cotransfected into HEK293T cells with wild-type miR-326 or its mutant. (**c**) Immunoblot analysis of hemagglutinin (HA) in HEK293T cells expressing a hemagglutinin-tagged wild-type Ets-1 3′ UTR construct (HA–Ets-1-3′ UTR) or Ets-1 3′ UTR with a mutated recognition element (3′ UTR-MRE), along with increasing dosages (wedge) of miR-326. (**d**) Expression of Ets-1 in $CD4^+$ T cells mock-transfected or transfected with LNA-anti-miR-326 or LNA-ctrl. (**e**–**i**) Immunoblot analysis and quantification of Ets-1 protein in $CD4^+$ T cells from lentivirus-infected mice (**e**), naive mice or mice with EAE (**f**,**g**) and clinical samples from controls and patients with relapsing multiple sclerosis (**h**,**i**). (**j**) Clinical scores of EAE in mice coinfected with various lentivirus combinations ($n = 5$ mice per group). LV-RFP, lentivirus expressing red fluorescent protein. (**k**) Immunoblot analysis of Ets-1 expression in splenocytes from the mice in **j**. (**l**) Intracellular cytokine staining of CNS infiltrates from the mice in **j**. Numbers in quadrants indicate percent $IL\text{-}17^+IFN\text{-}\gamma^-$ cells (top left) or $IL\text{-}17^-IFN\text{-}\gamma^+$ cells (bottom right) in the $CD4^+$ gate. (**m**) Quantification of CNS T_H-17 cells from the mice in **j**. Actin serves as a loading control throughout. $^*P < 0.05$, $^{**}P < 0.01$ and $^{***}P < 0.005$, versus control (Student's *t*-test). Data are from three (**b**,**c**,**e**–**i**), six (**d**) or four (**j**–**m**) independent experiments (mean and s.e.m. in **b**,**d**,**g**,**i**,**j**,**m**).

used microRNA inhibitor LNA-anti-miR-326 (a locked nucleic acid–modified antisense oligonucleotide directed against miR-326) produced an inhibitory effect on T_H-17 differentiation similar to that of infection with LV-sponge (**Fig. 4g–i**). We also differentiated T_H-17 cells *in vitro* with a bicistronic retrovirus encoding miR-326, an internal ribosomal entry site and GFP. Relative to infection by control retrovirus (encoding mutant miR-326), transduction of miR-326-encoding virus resulted in a substantially higher percentage of IL-17-expressing cells in the GFP^+ population, whereas infection with virus encoding a specific inhibitor of miR-326 resulted in a much lower percentage of IL-17-expressing GFP^+ cells. In contrast, these groups had a similar percentage of IL-17-producing cells among cells gated in the GFP^- population (**Supplementary Fig. 12**). Together these data demonstrate that miR-326 positively regulates T_H-17 differentiation both *in vivo* and *in vitro*.

To determine whether the effects of miR-326 on EAE development were due to its effect on T_H-17 differentiation, we infected mice with lentivirus and induced EAE. We collected splenocytes on day 14 after EAE induction and restimulated them *in vitro* for 96 h with MOG (35–55). We purified enriched MOG-specific $CD4^+$ T cells and transferred them into sublethally irradiated naive C57BL/6 mice by intravenous injection. The resultant EAE scores showed that mice given MOG-specific T cells from LV-326-infected donors had more severe disease, whereas mice transferred with LV-sponge-infected donor T cells showed less-severe signs. Thus, miR-326 expression by $CD4^+$ T cells strongly correlated with EAE development (**Supplementary Fig. 13**).

Ets-1 is a functional target of miR-326

We then applied the prediction programs TargetScan[28] and miRanda[29] to identify the potential miR-326 targets. Two reported negative regulators of T_H-17 differentiation, Ets-1 (ref. 7) and Foxp3 (A002750)[6], have putative miR-326-binding elements in their 3′ untranslated regions (UTRs). We found that miR-326 inhibited the luciferase activity of a reporter containing the wild-type *Ets1* 3′ UTR but not that of a reporter with a mutated 3′ UTR unable to bind miR-326 (**Fig. 5a**,**b**). However, miR-326 did not inhibit the luciferase activity of the reporter containing the wild-type *Foxp3* 3′ UTR (**Supplementary Fig. 14a**,**b**), nor did miR-326 affect the TGF-β1-driven induction of Foxp3 in naive $CD4^+$ T cells isolated from mice infected with lentivirus expressing miR-326 or producing 'knockdown' of miR-326 (**Supplementary Fig. 14c**), which indicates that miR-326 specifically targets Ets-1. Consistent with that, miR-326 suppressed the expression of Ets-1 protein encoded by a wild-type *Ets1* 3′ UTR in a dose-dependent way (**Fig. 5c**). Manipulation of miR-326 in $CD4^+$ T cells by LNA-anti-miR-326, LV-326 or LV-sponge regulated the amount of endogenous Ets-1 protein but did not affect *Ets1* transcripts (**Fig. 5d**,**e**), which indicates that miR-326 functions at the translational level. Moreover, there was a similar inverse correlation between the

expression of miR-326 and Ets-1 in $CD4^+$ T cells from mice with EAE and those from patients with multiple sclerosis (**Fig. 5f–i**).

To directly prove that Ets-1 is a functional target of miR-326 in the pathogenesis of multiple sclerosis, we did 'rescue' experiments with an Ets-1-expressing lentivirus containing mutated sequence encoding the recognition element of miR-326 (LV–Ets-1–3′ UTR-MRE). Transduction with LV–Ets-1–3′ UTR-MRE produces *Ets1* mRNA that is resistant to miR-326-mediated translational inhibition. Compared with mice infected with LV-ctrl, mice infected with LV-326 showed aggravated EAE, whereas this aggravation was completely abrogated by coinfection with LV–Ets-1–3′ UTR-MRE. Thus, restoration of Ets-1 protein reversed the effect of miR-326 (**Fig. 5j**,**k**). Flow cytometry analysis of cytokine production by CNS-infiltrating $CD4^+$ T cells further supported the idea that Ets-1 is the functional target of miR-326 during T_H-17 differentiation and the pathogenesis of multiple sclerosis (**Fig. 5l**,**m**).

DISCUSSION

T_H-17 cells are critically involved in the pathogenesis of chronic autoimmune diseases, including multiple sclerosis[30], and regulators of T_H-17 differentiation are considered to have valuable potential for clinical applications in the diagnosis or treatment of this category of complicated immune disorders[31]. Here we have reported a microRNA (miR-326) that is critically involved in the pathogenesis of multiple sclerosis and EAE by regulating T_H-17 differentiation. We have shown that miR-326 expression in $CD4^+$ T cells correlated well with disease in patients with relapsing multiple sclerosis and, moreover, its inhibition substantially ameliorated disease severity in the EAE model. Mechanistically, we have proven that by targeting Ets-1, a known negative regulator of T_H-17 cells, miR-326 promoted the generation of T_H-17 cells both *in vivo* and *in vitro*, and this was reversed by the reintroducion of an *Ets1* gene generated to be resistant to miR-326 suppression.

Our data suggest miR-326 is a T_H-17-associated microRNA, on the basis of the following observations. First, miR-326 expression correlated well with IL-17 expression in patients with multiple sclerosis. Second, the FISH assay of miR-326 and *Il-17a* in $CD4^+$ T cells from patients with multiple sclerosis and their enrichment in $CCR6^+CD4^+$ T cells showed that the peripheral blood of patients with relapsing multiple sclerosis had more IL-17-expressing $CD4^+$ T cells, with high expression of miR-326 in these cells. Upregulation of miR-326 was associated only with multiple sclerosis, as patients with NMO, another CNS inflammatory disorder similar to multiple sclerosis but mediated by antoantibodies, showed no miR-326 upregulation in PBLs[32]. Third, in the *in vitro* differentiation model, T_H-17 cells had higher expression of miR-326 than did T_H1, T_H2 or inducible T_{reg} cells. Finally, miR-326 was functionally involved in T_H-17 differentiation both *in vitro* and *in vivo*. Our findings may provide a new target for manipulating the generation of T_H-17 cells in related diseases. Further exploration of the function of miR-326 in other cell types, especially those of the innate immune system, will be of great importance for understanding the cell-differentiation network of the immune system.

Generally, microRNAs are believed to function *in vivo* by targeting multiple functionally related proteins or a key protein target[33,34]. In the immune system, miR-181 controls T cell antigen receptor signaling strength during T cell maturation by downregulating a set of negative regulators[35], whereas miR-150, the hematopoiesis-specific microRNA, controls embryonic development and B cell differentiation by regulating a key target, c-Myb[36,37]. Our data suggest miR-326 regulates T_H-17 cells mainly by targeting Ets-1. As a functional miR-326 target, Ets-1 therefore represents a distinct regulator of T_H-17 differentiation. Although published work has shown that Ets-1 restrains T_H-17 differentiation without affecting the induction of RORγt[7], the lineage-defining transcription factor of T_H-17 cells, the mechanisms regulating its own expression and the physiological relevance of Ets-1 have remained largely unclear. Our study has now shown that Ets-1 expression was substantially downregulated by miR-326 in patients with relapsing multiple sclerosis. Moreover, the greater disease severity and greater number of T_H-17 cells in LV-326-infected mice was largely reversed by coinfection of these mice with lentivirus expressing *Ets1* with a mutated 3′ UTR. This indicates Ets-1 indeed acts as a key target of miR-326, at least in the development of EAE and multiple sclerosis.

The immunosuppressive drugs now approved for the clinical treatment of multiple sclerosis work mainly by increasing the frequency of T_{reg} cells or by changing the T_H1-T_H2 bias[38]. Drugs that target T_H-17 cells, however, have not yet been applied to multiple sclerosis therapy. We found that miR-326 was substantially downregulated in a group of patients after glucocorticoid treatment (data not shown), the routine therapy for patients with multiple sclerosis to relieve symptoms caused during an acute relapse[39], which indicates that miR-326 expression itself not only correlates well with disease severity and the relapsing phase of multiple sclerosis but also is under the regulation of disease-modifying drugs or environmental factors in patients with multiple sclerosis. Combined with the findings that specific and inversely correlated up- or downregulation of the expression of miR-326 and Ets-1 was easily detected in blood samples from patients with multiple sclerosis, our results suggest that this microRNA-protein pair is of potential value as a biomarker for the diagnosis of multiple sclerosis disease, assessment of its prognosis or evaluation of drug responses. Also, elucidation of the specific signals that regulate miR-326 expression in disease will deepen the knowledge of how this noncoding RNA–mediated mechanism contributes to the pathogenesis of multiple sclerosis and help to identify new therapeutic approaches by targeting miR-326 for multiple sclerosis treatment. In summary, miR-326 may serve as a new and valuable target for clinical applications in patients with multiple sclerosis.

METHODS

Methods and any associated references are available in the online version of the paper at http://www.nature.com/natureimmunology/.

Accession codes. UCSD-Nature Signaling Gateway (http://www.signaling-gateway.org): A000889 and A002750.

Note: Supplementary information is available on the Nature Immunology website.

ACKNOWLEDGMENTS

We thank C. Dong (Anderson Cancer Center, Houston) for retrovector RV-GFP; X. Liu (Shanghai Institute for Biological Sciences) for fluorescein isothiocyanate–conjugated antibody to mouse T cell antigen receptor γδ; C. Wu (Sun Yat-sen University) for phycoerythrin-conjugated antibody to human CCR6; J. Zhao, L. Wei, Y. Shi, Q. Jing and G. Gao for discussions; and J. Zou, S. Xin, X. Zeng and S. Chen for technical assistance. Supported by the Ministry of Science and Technology (2005CB522406 and 2009CB941100), the National Natural Science Foundation of China (30621091, 30625014, 30623003, 30871285, 90713047 and 90919028), the Shanghai Municipal Commission for Science and Technology (07PJ14099) and the Chinese Academy of Sciences (2007KIP204 and SIBS2008001).

AUTHOR CONTRIBUTIONS

C.D., C.L., J.K. and G.P. designed the study; C.D., C.L. and S.H. did the experiments; Z.Y. contributed to the bioinformatics analysis target prediction; Z.W., Z.L. and G.Z. provided clinical samples; G.P. supervised the project; and C.L., C.D. and J.K. contributed to the writing of the paper.

Published online at http://www.nature.com/natureimmunology/.
Reprints and permissions information is available online at http://npg.nature.com/reprintsandpermissions/.

1. Korn, T., Bettelli, E., Oukka, M. & Kuchroo, V.K. IL-17 and Th17 cells. *Annu. Rev. Immunol.* **27**, 485–517 (2009).
2. Dong, C. T_H17 cells in development: an updated view of their molecular identity and genetic programming. *Nat. Rev. Immunol.* **8**, 337–348 (2008).
3. Zhou, L. & Littman, D.R. Transcriptional regulatory networks in Th17 cell differentiation. *Curr. Opin. Immunol.* **21**, 146–152 (2009).
4. Veldhoen, M. *et al.* The aryl hydrocarbon receptor links T_H17-cell-mediated autoimmunity to environmental toxins. *Nature* **453**, 106–109 (2008).
5. Brustle, A. *et al.* The development of inflammatory T_H-17 cells requires interferon-regulatory factor 4. *Nat. Immunol.* **8**, 958–966 (2007).
6. Zhou, L. *et al.* TGF-β-induced Foxp3 inhibits T_H17 cell differentiation by antagonizing RORγt function. *Nature* **453**, 236–240 (2008).
7. Moisan, J., Grenningloh, R., Bettelli, E., Oukka, M. & Ho, I.C. Ets-1 is a negative regulator of Th17 differentiation. *J. Exp. Med.* **204**, 2825–2835 (2007).
8. Compston, A. & Coles, A. Multiple sclerosis. *Lancet* **359**, 1221–1231 (2002).
9. Frohman, E.M., Racke, M.K. & Raine, C.S. Multiple sclerosis–the plaque and its pathogenesis. *N. Engl. J. Med.* **354**, 942–955 (2006).
10. Kantarci, O.H. Genetics and natural history of multiple sclerosis. *Semin. Neurol.* **28**, 7–16 (2008).
11. Polman, C.H. *et al.* Diagnostic criteria for multiple sclerosis: 2005 revisions to the "McDonald Criteria". *Ann. Neurol.* **58**, 840–846 (2005).
12. Sospedra, M. & Martin, R. Immunology of multiple sclerosis. *Annu. Rev. Immunol.* **23**, 683–747 (2005).
13. Pettinelli, C.B. & McFarlin, D.E. Adoptive transfer of experimental allergic encephalomyelitis in SJL/J mice after in vitro activation of lymph node cells by myelin basic protein: requirement for $Lyt1^+2^-$ T lymphocytes. *J. Immunol.* **127**, 1420–1423 (1981).
14. Langrish, C.L. *et al.* IL-23 drives a pathogenic T cell population that induces autoimmune inflammation. *J. Exp. Med.* **201**, 233–240 (2005).
15. Ivanov, I.I. *et al.* The orphan nuclear receptor RORγt directs the differentiation program of proinflammatory $IL\text{-}17^+$ T helper cells. *Cell* **126**, 1121–1133 (2006).
16. Tzartos, J.S. *et al.* Interleukin-17 production in central nervous system-infiltrating T cells and glial cells is associated with active disease in multiple sclerosis. *Am. J. Pathol.* **172**, 146–155 (2008).
17. Bartel, D.P. MicroRNAs: target recognition and regulatory functions. *Cell* **136**, 215–233 (2009).
18. Ma, L., Teruya-Feldstein, J. & Weinberg, R.A. Tumour invasion and metastasis initiated by microRNA-10b in breast cancer. *Nature* **449**, 682–688 (2007).
19. Thum, T. *et al.* MicroRNA-21 contributes to myocardial disease by stimulating MAP kinase signalling in fibroblasts. *Nature* **456**, 980–984 (2008).
20. Lu, J. *et al.* MicroRNA expression profiles classify human cancers. *Nature* **435**, 834–838 (2005).
21. Slack, F.J. & Weidhaas, J.B. MicroRNA in cancer prognosis. *N. Engl. J. Med.* **359**, 2720–2722 (2008).
22. Zhou, X. *et al.* Selective miRNA disruption in T reg cells leads to uncontrolled autoimmunity. *J. Exp. Med.* **205**, 1983–1991 (2008).
23. Chong, M.M., Rasmussen, J.P., Rudensky, A.Y. & Littman, D.R. The RNAseIII enzyme Drosha is critical in T cells for preventing lethal inflammatory disease. *J. Exp. Med.* **205**, 2005–2017 (2008).
24. Wingerchuk, D.M., Lennon, V.A., Lucchinetti, C.F., Pittock, S.J. & Weinshenker, B.G. The spectrum of neuromyelitis optica. *Lancet Neurol.* **6**, 805–815 (2007).
25. Acosta-Rodriguez, E.V. *et al.* Surface phenotype and antigenic specificity of human interleukin 17-producing T helper memory cells. *Nat. Immunol.* **8**, 639–646 (2007).
26. Ebert, M.S., Neilson, J.R. & Sharp, P.A. MicroRNA sponges: competitive inhibitors of small RNAs in mammalian cells. *Nat. Methods* **4**, 721–726 (2007).
27. Pan, D. *et al.* Biodistribution and toxicity studies of VSVG-pseudotyped lentiviral vector after intravenous administration in mice with the observation of in vivo transduction of bone marrow. *Mol. Ther.* **6**, 19–29 (2002).
28. Lewis, B.P., Shih, I.H., Jones-Rhoades, M.W., Bartel, D.P. & Burge, C.B. Prediction of mammalian microRNA targets. *Cell* **115**, 787–798 (2003).
29. John, B., Sander, C. & Marks, D.S. Prediction of human microRNA targets. *Methods Mol. Biol.* **342**, 101–113 (2006).
30. Tesmer, L.A., Lundy, S.K., Sarkar, S. & Fox, D.A. Th17 cells in human disease. *Immunol. Rev.* **223**, 87–113 (2008).
31. Miossec, P., Korn, T. & Kuchroo, V.K. Interleukin-17 and type 17 helper T cells. *N. Engl. J. Med.* **361**, 888–898 (2009).
32. Lennon, V.A. *et al.* A serum autoantibody marker of neuromyelitis optica: distinction from multiple sclerosis. *Lancet* **364**, 2106–2112 (2004).
33. Xiao, C. & Rajewsky, K. MicroRNA control in the immune system: basic principles. *Cell* **136**, 26–36 (2009).
34. Hoefig, K.P. & Heissmeyer, V. MicroRNAs grow up in the immune system. *Curr. Opin. Immunol.* **20**, 281–287 (2008).
35. Li, Q.J. *et al.* miR-181a is an intrinsic modulator of T cell sensitivity and selection. *Cell* **129**, 147–161 (2007).
36. Lin, Y.C. *et al.* c-Myb is an evolutionary conserved miR-150 target and miR-150/c-Myb interaction is important for embryonic development. *Mol. Biol. Evol.* **25**, 2189–2198 (2008).
37. Xiao, C. *et al.* MiR-150 controls B cell differentiation by targeting the transcription factor c-Myb. *Cell* **131**, 146–159 (2007).
38. Schrempf, W. & Ziemssen, T. Glatiramer acetate: mechanisms of action in multiple sclerosis. *Autoimmun. Rev.* **6**, 469–475 (2007).
39. Brusaferri, F. & Candelise, L. Steroids for multiple sclerosis and optic neuritis: a meta-analysis of randomized controlled clinical trials. *J. Neurol.* **247**, 435–442 (2000).

ONLINE METHODS

Study subjects. Subjects were patients from the outpatient clinic of Huashan Hospital (Shanghai, China) with clinically defined RRMS or NMO or age- and sex-matched healthy volunteers from personnel of the Institute of Biochemistry and Cell Biology. Blood samples were obtained from subjects after informed consent was provided and the sampling was completed in accordance with the guidelines of local institutional review boards.

Mice. C57BL/6 mice were from the Shanghai Laboratory Animal Center (Chinese Academy of Sciences). Protocols for animal experiments were approved by the institutional animal use committee of the Shanghai Institutes for Biological Sciences (Chinese Academy of Sciences). All mice were maintained in pathogen-free conditions.

Reagents. The following antibodies were from BD Pharmingen: fluorescein isothiocyanate–conjugated anti–mouse CD3ξ (145-2C11), anti–mouse CD4 (L3T4), anti–mouse CD8a (53-6.7), anti–mouse CD19 (1D3) and anti–mouse CD62L (MEL-14); phycoerythrin-conjugated anti–mouse CD45R (B220; RA3-6B2) and anti–mouse IL-17 (TC11-18H10.1); phycoerythrin–cyanine 5.5–conjugated anti–mouse CD44 (IM7); and anti-CD16-CD32 (2.4G2). Phycoerythrin-indotricarbocyanine–conjugated anti–mouse CD4 (L3T4), allophycocyanin-conjugated anti–mouse IFN-γ (XMG1.2), phycoerythrin-conjugated anti-Foxp3 (FJK-16S) and allophycocyanin-conjugated anti–human CD4 (eBio64DEC17) were from eBiosciences. Secondary antibodies anti-Ets-1 (sc-350; Santa Cruz) and IRDye 800CW–conjugated affinity-purified anti–rabbit immunoglobulin G (600-431-384; Rockland) were used for immunoblot analysis.

Lentivirus-mediated overexpression or inhibition of miR-326. A genomic sequence spanning the mouse miR-326 coding region flanked by approximately 100 base pairs from 5′ or 3′ on either end was cloned into lentivral vector pCDH-CMV-MCS-EF1-copGFP (CD511B-1; System Bioscience) downstream of the cytomegalovirus promoter. For control or miR-326 inhibition, sequence encoding mutant miR-326 or its specific inhibitor (sponge) was cloned into the same vector. Virus was produced and target cells were infected according to the user's manual.

T cell purification and activation. Naive $CD4^+CD62L^+$ helper T cells were prepared by magnetic cell sorting from spleens of female C57BL/6 mice 6–8 weeks of age. Sorted cells were activated with anti-CD3 (2 μg/ml; 145-2C11, soluble; BD Pharmingen) and anti-CD28 (2 μg/ml; 37.51, soluble; BD Pharmingen) and were induced to differentiate into T_H1 cells by supplementation with IL-12 (10 ng/ml; Peprotech) plus anti-IL-4; into T_H2 cells with IL-4 (40 ng/ml plus anti-IFN-γ; or into inducible T_{reg} cells with TGF-β1 (5 ng/ml; Peprotech) and recombinant mouse IL-2 (50 U/ml; peprotech) plus anti-IFN-γ. Cells stimulated in 'neutral' conditions (anti-IL-4 plus anti- IFN-γ but no additional cytokines) were considered 'T_H0' cells. For T_H-17 differentiation, cells usually received anti-IL-4 and anti-IFN-γ plus a T_H-17 'cocktail' containing TGF-β1 (3 ng/ml), IL-6 (30 ng/ml; eBioscience), tumor necrosis factor (10 ng/ml; Peprotech) and IL-1β (10 ng/ml; Peprotech). Neutralizing anti-IFN-γ (XMG1.2; BD Pharmingen) and anti-IL-4 (11B11; BD Pharmingen) were each used at a concentration of 10 μg/ml.

EAE. The encephalitogenic peptide MOG (35–55) (GLBiochem) used to induce EAE had a purity of 95%. For EAE induction, female C57BL/6 mice 6–8 weeks of age were immunized subcutaneously with 150 μg MOG (35–55) in complete Freund's adjuvant containing heat-killed *Mycobacterium tuberculosis* (H37Ra strain; 5 mg/ml; BD Diagnostics). Pertussis toxin (200 ng per mouse; Calbiochem) in PBS was administered intraperitoneally on day 0 and day 2. Mice were examined daily for disease signs by researchers 'blinded' to experimental conditions and were assigned scores on a scale of 0–5 as follows[40]: 0, no clinical signs; 1, paralyzed tail; 2, paresis (weakness, incomplete paralysis of one or two hindlimbs); 3, paraplegia (complete paralysis of both hindlimbs); 4, paraplegia with forelimb weakness or paralysis; and 5, moribund state or death. For analysis of central nervous system infiltrates, brain and spinal cord tissues were collected from perfused mice and mononuclear cells were prepared by Percoll gradient centrifugation. For histological analysis, the same tissue samples were immediately fixed in 4% (wt/vol) paraformaldehyde. Paraffin-embedded sections of spinal cord were stained with hematoxylin and eosin or with Luxol fast blue for analysis of inflammation or demyelination, respectively.

Intracellular staining and flow cytometry. For intracellular cytokine staining, cells obtained from *in vitro* culture or from DLNs or CNS infiltrates of mice with EAE were incubated in a tissue culture incubator for 5 h at 37 °C with phorbol 12-myristate 13-acetate (50 ng/ml; Sigma), ionomycin (750 ng/ml; Sigma) and brefeldin A (10 μg/ml; Sigma). Surface staining was done as described above with the corresponding fluorescence-labeled surface antibodies. After surface staining, cells were resuspended in Fixation/Permeabilization solution (Cytofix/Cytoperm kit; BD Pharmingen) and intracellular cytokine staining was done according to the manufacturer's protocol. For Foxp3 staining, cells were not stimulated with phorbol 12-myristate 13-acetate and ionomycin; instead, the protocol for the Foxp3 Staining Buffer set was followed (eBioscience). A FACSCalibur and CellQuest software or an LSR II and FACSDiva (BD Biosciences) were used for flow cytometry.

Oligonucleotide transfection. An antisense oligonucleotide modified by locked nucleotide acid (LNA; Dharmacon) was synthesized to inhibit miR-326. Primary mouse $CD4^+$ T cells were transfected by nucleofection (program X-01; Amaxa) with 50 nM LNA-anti-miR-326 or the 'scrambled' control at 20 h after activation.

Luciferase reporter assay. HEK293T cells (American Type Culture Collection) were maintained in DMEM (Gibco-BRL) and cells of 50% confluence in 24-well plates were transfected with Fugene HD reagent (Roche). A firefly luciferase reporter gene construct (200 ng per well) and pRL-SV40 Renilla luciferase construct (1 ng per well; for normalization) were cotransfected. Cell extracts were prepared 24 h after transfection and luciferase activity was measured with the Dual-Luciferase Reporter Assay system (Promega). Wild-type or mutated 3′ UTR sequences of *Ets1* or *Smo* (encoding smoothened) were cloned into the modified pGL3-control vector (Promega) as described[41].

ELISA. Cytokines in culture supernatants after *in vitro* stimulation were quantified by ELISA according to the manufacturer's instructions as follows: for mouse IL-17 and IFN-γ, R&D Systems; for mouse TGF-β1, Genetimes Technology.

Statistics. A two-tailed Student's *t*-test was applied for statistical comparison of two groups, or where appropriate, the two-way analysis of variance followed by Bonferroni's post-hoc test for multiple comparisons and a Mann–Whitney test for nonparametric data (EAE scoring). A P value of 0.05 or less was considered significant.

40. Stromnes, I.M. & Goverman, J.M. Active induction of experimental allergic encephalomyelitis. *Nat. Protoc.* **1**, 1810–1819 (2006).
41. Chen, J.F. *et al.* The role of microRNA-1 and microRNA-133 in skeletal muscle proliferation and differentiation. *Nat. Genet.* **38**, 228–233 (2006).

doi:10.1038/ni.1798